# Condition Monitoring and Fault Diagnosis of a Rotary Machine using Fast Fourier Transform (FFT) Analysis

[1]Akshay Joshi, [2]N. S. Nagmoti, [3]M. M. Khot

[1]Student, [2]Assistant Professor, [3]Assistant Professor
[1]Mechanical Engineering Department,
[1]Walchand College of Engineering, Sangli, India

***Abstract:*** This work has been undertaken for the condition monitoring of the rotary machine and thereby to diagnose the fault present in it. The analysis technique used for condition monitoring is Fast Fourier Transform (FFT) using three axis accelerometer sensors. The fault present in the rotary machine setup has been successfully detected by FFT analysis with the help of vibrometer readings and FFT spectra obtained from accelerometer sensors at different rotational speeds.

***Keywords* – Condition monitoring, fault diagnosis, FFT, vibration analysis, rotary machine.**

## 1. INTRODUCTION

Different types of machines are present in the industry. The majority of these machines have rotating components. The rotating machinery is one of the most important equipment in modern industrial applications. Unexpected failures of rotating machinery may endanger normal machine operation, machine efficiency and machine life and thus cause significant economic losses. Therefore, condition monitoring and fault diagnosis of rotating machinery play an important role in terms of system maintenance and process automation. For this purpose, vibration analysis is usually used since vibration signals are easy to gather and are highly correlative with the working conditions of rotating machinery [7].

Machinery condition monitoring deals with the maintenance aspects of these machines based on the present and past conditions of the machine. In order to understand the machine's condition, sensors are installed on the different components of the machine; so that relevant data about the machine's health can be collected, analyzed and decisions made regarding the appropriate maintenance or necessary actions to be taken so that the machine is able to perform as per its original design objectives [1].

Fast Fourier Transform (FFT) analysis is an incredibly helpful method for machinery condition monitoring. If a machinery problem exists, FFT spectra provide information to diagnose the fault present in the machinery. FFT spectra gives the information about vibration amplitudes at various speeds on the FFT spectrum. In this way, we can identify and track vibrations occurring at specific frequencies. Since we know that certain machinery problems generate excessive vibrations at specific frequencies, we can use this information to diagnose the reason for these excessive vibrations [5].

In this paper, the experimental results regarding the rotary machine based on the vibration FFT spectra are presented. It aims to monitor the condition of the rotary machine and diagnose the fault present in the rotary machine with different rotational speeds at real-time.

## 2. FAST FOURIER TRANSFORM (FFT)

A vibration or a system response can be represented by displacement, velocity and acceleration in both time and frequency domains. Time domain consists of amplitude which varies with time. This time domain signal is referred to as filter-out or overall reading. Frequency domain is the domain where amplitudes are represented as series of sine and cosine waves. These waves consists of a magnitude and a phase, which vary with frequency. The measured vibrations are primarily in analog form i.e. time domain and are required to be transformed to the frequency domain. This is the purpose of the Fast Fourier transform (FFT) analysis.

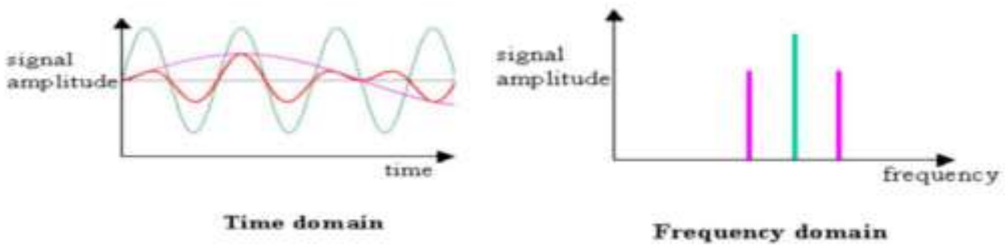


Figure 1. Time Domain and Frequency Domain [1]

The vibration of a machine is a physical motion. Vibration sensors convert this motion into an electrical signal. The electrical signal is then sent to data collectors or analyzers. The analyzers then process this signal to give the FFT spectra.

## 3. MISALIGNMENT

Misalignment is created when meeting shafts, couplings and bearings are not properly aligned along their centerlines. There are three types of misalignment. They are angular misalignment, parallel misalignment or a combination of both.

### 3.1 ANGULAR MISALIGNMENT

Angular misalignment primarily causes the driver and driven machine shafts to vibrate at the 1X rpm frequency in axial direction. But pure angular misalignment is rare. There will be high axial vibrations with both 1X rpm and 2X rpm. A phase difference of 180° will be observed across the coupling in case of angular misalignment.

### 3.2 PARALLEL MISALIGNMENT

Parallel misalignment results in 2X rpm vibrations in the radial direction. Parallel misalignment has similar vibrations symptoms compared to angular misalignment; but for high radial vibrations, a phase difference of 180° will be observed across the coupling. Pure parallel misalignment is rare and is commonly observed to be in combination with angular misalignment. Thus, we will see both the 1X rpm and 2X rpm peaks.

## 4. EXPERIMENTAL SETUP

Experimental setup consists of a three phase induction motor (3 HP), discs, bearing pedestal, coupling and a shaft. Experimental setup is mounted on the concrete support. Discs have arrangement for balancing. Figure 2 below shows the experimental setup.

**Test setup information:**

- Havells – Lafert Motors
- Energy Efficient 3ø Induction Motor
- Power: 2.2 KW (3 HP)
- RPM: 1435 rpm
- Amp: 5.22 A
- Volt: 415 (+/-) 5 Volts
- Frequency: 50 (+/-) 5 % Hz
- Efficiency: 0.83

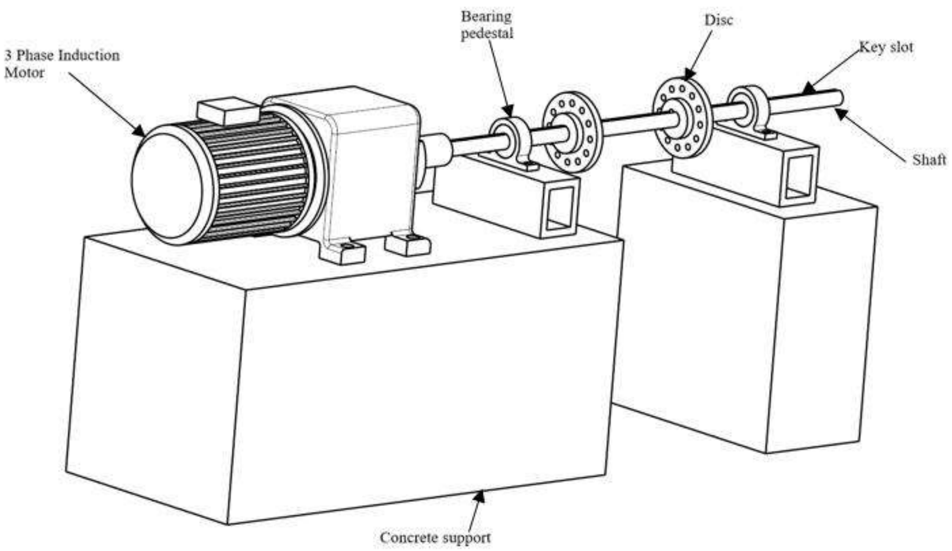


Figure 2. Experimental Setup

**Data Acquisition System:**

- CEMB N600 Dual Channel Vibrometer and Spectrum Analyzer
- Dual Channel Vibrometer
- Spectrum Analyzer
- Portable Equipment

## 5. READINGS

Figure 3 below shows the sensors in three different directions. Horizontal and vertical directions represent radial plane; whereas axial direction represents the axial plane.

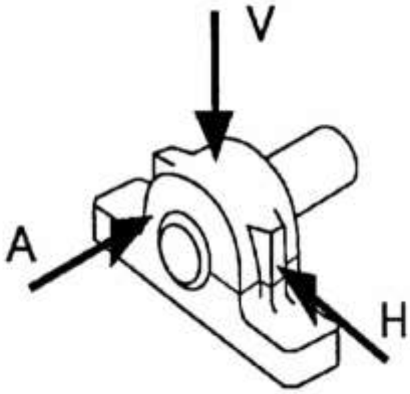


Figure 3. Sensor Directions in different planes

- H: Horizontal Direction
- V: Vertical Direction
- A: Axial Direction

Figure 4 and Figure 5 shows the experimental setup with sensors connected in horizontal and vertical directions at driving end and non-driving end respectively.

Figure 4. Sensors in Horizontal Direction

Figure 5. Sensors in Vertical Direction

Figure 6. Accelerometer in Horizontal plane

Figure 7. Accelerometer in Vertical plane

## 6. RESULTS AND DISCUSSION

### i. AT 800 RPM IN HORIZONTAL DIRECTION

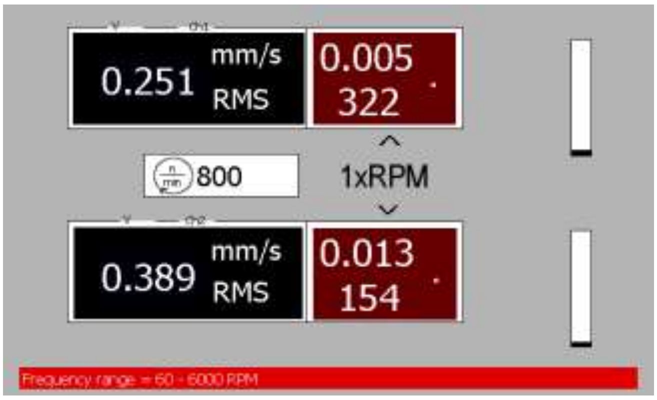


Figure 8. Vibrometer reading at 800 rpm in Horizontal Plane

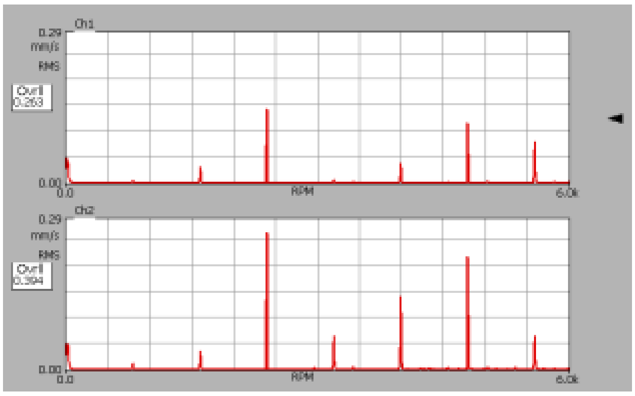


Figure 9. FFT graph at 800 rpm in Horizontal plane

| Ch1 mm/s RMS | Freq [RPM] |
|---|---|
| 0.143 | 2399 |
| 0.116 | 4798 |
| 0.082 | 5598 |
| 0.050 | 10 |
| 0.040 | 3998 |
| 0.031 | 1599 |
| 0.006 | 3199 |
| 0.005 | 800 |
| 0.003 | 5027 |
| 0.002 | 3427 |

Figure 10. Peak list of Driving End

| Ch2 mm/s RMS | Freq [RPM] |
|---|---|
| 0.262 | 2399 |
| 0.215 | 4798 |
| 0.145 | 3998 |
| 0.067 | 3199 |
| 0.066 | 5598 |
| 0.050 | 11 |
| 0.036 | 1599 |
| 0.012 | 800 |
| 0.005 | 3428 |
| 0.004 | 4228 |

Figure 11. Peak list of Non-Driving End

### ii. AT 800 RPM IN VERTICAL DIRECTION


Figure 12. Vibrometer reading at 800 rpm in Vertical Plane

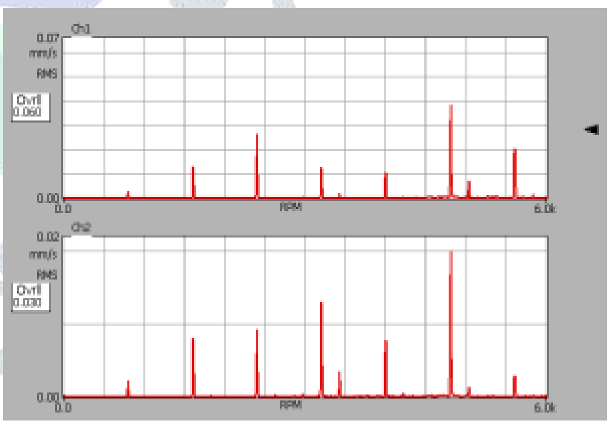


Figure 13. FFT graph at 800 rpm in Vertical plane

| Ch1 mm/s RMS | Freq [RPM] |
|---|---|
| 0.040 | 4811 |
| 0.027 | 2405 |
| 0.022 | 5612 |
| 0.013 | 1604 |
| 0.013 | 3207 |
| 0.011 | 4009 |
| 0.007 | 5038 |
| 0.003 | 802 |
| 0.002 | 3435 |
| 0.002 | 5841 |

Figure 14. Peak list of Driving End

| Ch2 mm/s RMS | Freq [RPM] |
|---|---|
| 0.021 | 4810 |
| 0.013 | 3207 |
| 0.009 | 2405 |
| 0.008 | 1604 |
| 0.008 | 4009 |
| 0.003 | 3435 |
| 0.003 | 5612 |
| 0.002 | 802 |
| 0.001 | 5040 |
| 0.001 | 4832 |

Figure 15. Peak list of Non-Driving End

### iii. AT 800 RPM IN AXIAL DIRECTION


Figure 16. Vibrometer reading at 800 rpm in Axial Plane

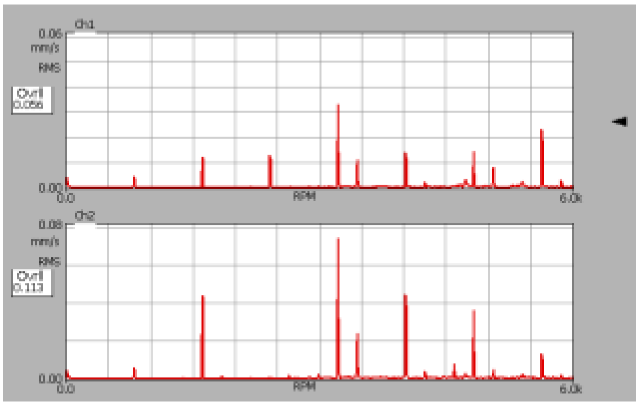


Figure 17. FFT graph at 800 rpm in Axial Plane

| Ch1 mm/s RMS | Freq [RPM] |
|---|---|
| 0.033 | 3223 |
| 0.024 | 5640 |
| 0.015 | 4028 |
| 0.015 | 4835 |
| 0.014 | 2417 |
| 0.012 | 1612 |
| 0.012 | 3454 |
| 0.009 | 5064 |
| 0.005 | 806 |
| 0.004 | 9 |

Figure 18. Peak list of Driving End

| Ch2 mm/s RMS | Freq [RPM] |
|---|---|
| 0.074 | 3223 |
| 0.047 | 4028 |
| 0.044 | 1612 |
| 0.036 | 4835 |
| 0.025 | 3454 |
| 0.014 | 5640 |
| 0.008 | 4603 |
| 0.006 | 806 |
| 0.005 | 5067 |
| 0.005 | 9 |

Figure 19. Peak list of Non-Driving End

### iv. AT 600 RPM IN HORIZONTAL DIRECTION


Figure 20. Vibrometer reading at 600 rpm in Horizontal Plane

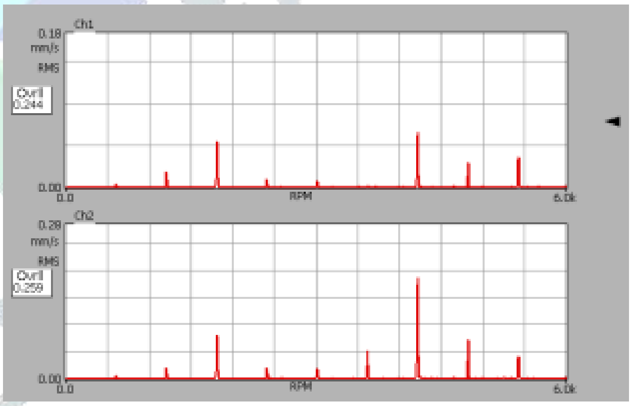


Figure 21. FFT graph at 600 rpm in Horizontal Plane

| Ch1 mm/s RMS | Freq [RPM] |
|---|---|
| 0.071 | 4225 |
| 0.060 | 1811 |
| 0.039 | 5432 |
| 0.029 | 4828 |
| 0.018 | 1207 |
| 0.009 | 2414 |
| 0.008 | 3018 |
| 0.003 | 604 |
| 0.002 | 5001 |
| 0.002 | 3623 |

Figure 22. Peak list of Driving End

| Ch2 mm/s RMS | Freq [RPM] |
|---|---|
| 0.200 | 4225 |
| 0.087 | 1811 |
| 0.071 | 4828 |
| 0.050 | 3621 |
| 0.044 | 5432 |
| 0.021 | 2414 |
| 0.020 | 1207 |
| 0.020 | 3018 |
| 0.005 | 604 |
| 0.004 | 5000 |

Figure 23. Peak list of Non-Driving End

### v. AT 600 RPM IN VERTICAL DIRECTION


Figure 24. Vibrometer reading at 600 rpm in Vertical Plane

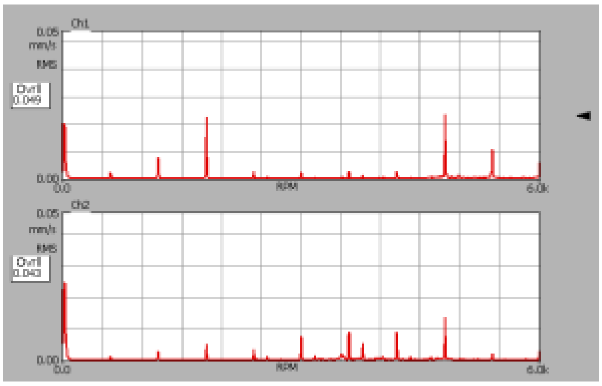


Figure 25. FFT graph at 600 rpm in Vertical Plane

| Ch1 mm/s RMS | Freq [RPM] |
|---|---|
| 0.023 | 4814 |
| 0.023 | 1806 |
| 0.020 | 17 |
| 0.011 | 5415 |
| 0.008 | 1204 |
| 0.003 | 3611 |
| 0.002 | 2407 |
| 0.002 | 601 |
| 0.002 | 4212 |
| 0.002 | 3008 |

Figure 26. Peak list of Driving End

| Ch2 mm/s RMS | Freq [RPM] |
|---|---|
| 0.025 | 20 |
| 0.013 | 4814 |
| 0.010 | 3611 |
| 0.009 | 4212 |
| 0.008 | 3008 |
| 0.005 | 3784 |
| 0.005 | 1806 |
| 0.003 | 2407 |
| 0.003 | 1204 |
| 0.002 | 3516 |

Figure 27. Peak list of Non-Driving End

### vi. AT 600 RPM IN AXIAL DIRECTION

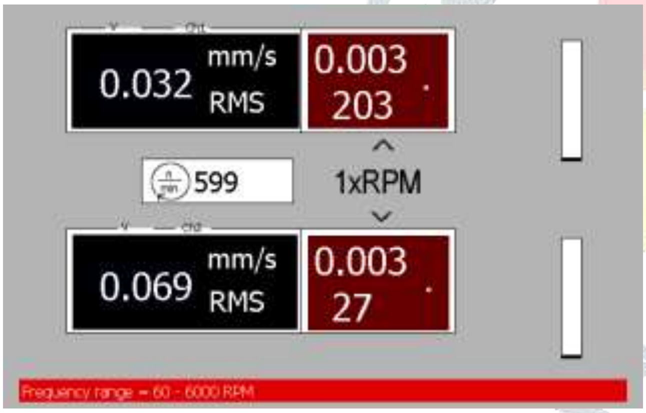


Figure 28. Vibrometer reading at 600 rpm in Axial Plane

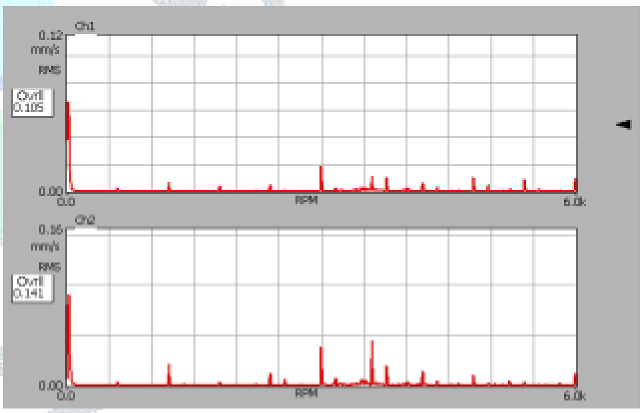


Figure 29. FFT graph at 600 rpm in Axial Plane

| Ch1 mm/s RMS | Freq [RPM] |
|---|---|
| 0.067 | 13 |
| 0.019 | 2998 |
| 0.011 | 3598 |
| 0.010 | 4797 |
| 0.010 | 3770 |
| 0.009 | 5396 |
| 0.007 | 1199 |
| 0.006 | 4197 |
| 0.005 | 2398 |
| 0.005 | 4969 |

Figure 30. Peak list of Driving End

| Ch2 mm/s RMS | Freq [RPM] |
|---|---|
| 0.091 | 21 |
| 0.044 | 3598 |
| 0.038 | 2998 |
| 0.021 | 1199 |
| 0.019 | 3771 |
| 0.014 | 4197 |
| 0.012 | 2398 |
| 0.010 | 4797 |
| 0.008 | 3170 |
| 0.006 | 2571 |

Figure 31. Peak list of Non-Driving End

From the above vibrometer readings at 800 rpm and 600 rpm, we can observe that there is a phase difference of 180° (±30°) between driving end and non-driving end in horizontal direction and vertical direction i.e. in radial plane and also in axial direction i.e. in axial plane [ISO 2372].

We can observe 1X and 2X frequencies along with multiple harmonics from 3X to 10X in FFT spectra data at 800 rpm and 600 rpm in both radial and axial planes [ISO 2372].

## 7. CONCLUSION

In this work, the condition monitoring of the rotary machine setup has been performed and thereby the fault present in the system has been diagnosed with the help of Fast Fourier Transform analysis. The vibrometer readings and FFT spectra data at 800 rpm and 600 rpm show that there is a Combination of Parallel and Angular Misalignment fault present in the rotary machine setup.

## 8. REFERENCES

**[1]** Amiya R. Mohanty, "Machinery condition monitoring principles and practices," *Indian Institute of Technology Mechanical Engineering Department, Kharagpur, West Bengal, India.*

**[2]** Giovanni Betta, Consolatina Liguori, Alfredo Paolillo, Antonio Pietrosanto "A IMP- based FFT-Analyzer for the Fault Diagnosis of Rotating Machine based on Vibration Analysis," *IEEE Instrumentation and Measurement Technology Conference Budapest, Hungary, 0-7803-6646-81, May 2001.*

**[3]** R.J.E. Merry, "Wavelet Theory and Applications, a literature study" *Eindhoven University of Technology, Department of Mechanical Engineering.*

**[4]** Issam Atoui, H. Meradi, R. Boulkroune, R. Saidi and A. Grid, "Fault detection and diagnosis in rotating machinery by vibration monitoring using FFT and Wavelet techniques", (2013) *8th International Workshop on Systems, Signal Processing and their Applications (WoSSPA)*, Algiers, 2013, pp. 401-406, doi: 10.1109/WoSSPA.2013.6602399.

**[5]** Jason Mais, "Spectrum Analysis the key features of analyzing spectra," *SKF USA Inc.*

**[6]** SKF Reliability Systems, "Vibration Diagnostic Guide," *SKF USA Inc.*

**[7]** Peng Li, Fanrang Kong, Qingbo He, Yongbin Liu, "Multiscale slope feature extraction for rotating machinery fault diagnosis using wavelet analysis," *Department of Precision Machinery and Precision Instrumentation, University of Science and Technology of China, Hefei, Anhui 230026, PR China.*